Yang Gao*, Miriam Weiß, and Werner Nahm

Reduction of Uncertainty in Bolus Transit Time Measurement in Quantitative Fluorescence Angiography

https://doi.org/10.1515/cdbme-2023-1155

Abstract: During cerebral revascularization surgeries, blood flow values help surgeons to monitor the quality of the procedure, e.g., to avoid cerebral hyperperfusion syndrome due to excessively enhanced perfusion. The state-of-the-art technique is the ultrasonic flow probe that has to be placed around the blood vessel. This causes contact between probe and vessel, which, in the worst case, leads to rupture. The recently developed intraoperative indocyanine green (ICG) Quantitative Fluorescence Angiography (QFA) is an alternative technique that overcomes this risk. However, it has been shown by the developer that the calculated flow has deviations. After determining the bolus transit time as the most sensitive parameter in flow calculation, we propose a new two-step uncertainty reduction method for flow calculation. The first step is to generate more data in each measurement that results in functions of the parameters. Noise can then be reduced in a second step. Two methods for this step are compared. The first method fits the model for each parameter function separately and calculates flow from models, while the second one fits multiple parameter functions together. The latter method is proven to perform best by *in silico* tests. Besides, this method reduces the deviation of flow comparing to original QFA as expected. Our approach can be generally used in all QFA applications using two-point theory. Further development is possible if number of dimensions of the achieved parameter data are broadened that results in even more data for processing in the second step.

Keywords: ICG, Quantitative Fluorescence Angiography, QFA, neurosurgery, non-contact, blood flow measurement, uncertainty reduction.

1 Introduction

Even though the brain is a rather small organ, it consumes a huge amount of energy that is transported by blood [1]. To maintain brain function, patients undergoing hypoperfusion may need revascularization surgeries to restore a proper blood flow function [2, 3]. By measuring the blood flow intraoperatively, better surgical outcomes are observed, e.g., cerebral hyperperfusion syndrome (CHS) caused by exceeded perfusion enhancement through surgeries can be avoided or occurrence can be reduced [2–5]. The state-of-the-art technique for this measurement is ultrasonic (US) flow probe. However, it may cause contamination, compromise and rupture due to the contact between device and vessel [4]. Thus, the optical camera-based alternative, Quantitative Fluorescence Angiography (QFA), has been implemented by Ady Naber [6]. In this method, flow is generally dependent on injected bolus transit distance, time and cross section area of the blood vessel. The resulting calculated flow is, however, deviated and thus, in a certain range due to e.g., camera noise, heart pulse and non-uniformly distributed fluorescence particles. Multiple tests on this system reveal that transit time is the most sensitive parameter. Thus, reliable flow strongly correlates with transit time uncertainty reduction. Calculating average flow values by taking multiple measurements is not feasible in QFA due to the need for repeated dye injections, which would significantly increase time requirements and render it impractical for intraoperative use. Hence, the aim of this work is to provide a method for transit time uncertainty reduction that results in more reliable flow measurements even if cause and distribution of this uncertainty is unclear.

2 Quantitative Fluorescence Angiography

QFA is a method that calculates blood flow in a certain area of the blood vessel. Therefore, solution including fluorescence dye is injected into blood veins. The dye reaches the brain through blood transport. Flow can then be calculated through dye concentration over time that is approximated by fluorescence intensity. In our work, QFA is based on two-point theory whose basic principles are shown in Figure 1. The physical assumption of QFA is an approximately constant cross section area and a constant velocity anywhere between the two defined points (here **A** and **B**). In this case, flow can be derived from

***Corresponding author: Yang Gao,** Karlsruhe Institute of Technology, Institute of Biomedical Engineering, 30.33, Karlsruhe, Germany, e-mail: Sebastiangao1230@gmail.com
Miriam Weiß, Werner Nahm, Karlsruhe Institute of Technology, Institute of Biomedical Engineering, 30.33, Karlsruhe, Germany

the bolus travel distance and transit time, Δs and Δt, respectively, as well as the cross section area of the blood vessel, A:

$$\dot{V} = \frac{\Delta s}{\Delta t} \cdot A. \tag{1}$$

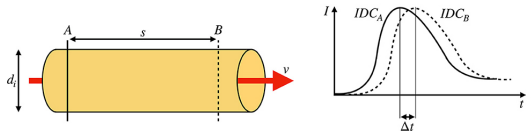

Fig. 1: Two-point measurement of QFA. Δt is calculated through the shift of the Indicator Dilution Curves (IDCs), which are estimated based on the light intensity from the two regions of interest (ROIs) at manually selected points **A** and **B**. [7]

The vessel of interest must be segmented first. Afterwards, a centerline corresponding to the mask will be calculated automatically. Figure 2 shows an example of the segmentation mask (white area) and its centerline (black line in the middle).

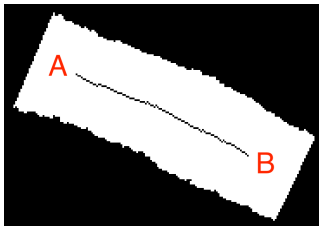

Fig. 2: Segmentation mask and its centerline. Based on it, three parameters for flow calculation can be derived.

Δs represents the length of the centerline. Circles with increasing diameter whose middle point is a pixel of the centerline will be placed virtually in the mask until they hit the edge. Then, the diameter d can be estimated. The cross section area A is calculated through the diameter as follows:

$$A = \frac{\pi}{4} \cdot \sum_{i=1}^{n} d_i^2, \tag{2}$$

where n is the number of pixels in the centerline. The calculation of Δt only depends on the two endpoints of the centerline. The region of interest (ROI) at each endpoint is defined as a square with a side length equal to one-third of the diameter of the endpoint, and the endpoint itself serves as the center of the square. To create an Indicator Dilution Curve (IDC), the mean value of all pixels within each ROI is calculated. The two resulting IDCs will be normalized by their respective maximum values, and five methods will be used to calculate the time difference Δt between them. This paper will focus on two of these methods, described in more detail in [6], for the sake of visualization:

– **raw1**. Δt is the mean value of x-axis value shift when setting y-axis target value to 2 %, 3 %, 4 %, 5 %, 7 %, 10 %.
– **ldrw**. Model Local Density Random Walk (LDRW) will be fit to both entire signals. Then, the cross correlation between the two models will be calculated. Δt corresponds to the shift where the cross correlation function reaches its maximum.

3 Methods

The data used in this work consists of 17 patient videos and intraoperatively recorded flow values from an US flow probe. As the exact position of the US measurement is uncertain and its deviation itself, the US flow values are used as a reference rather than a ground truth. Computational implementation and visualization is realized with Matlab R2021a [8].

The main difficulty in uncertainty reduction is the data acquisition. QFA derives only one flow value per run, as it depends on a single calculation for each of the three parameters ($\Delta s, \Delta t, A$). Centerline shortening addresses this limitation by modifying the selected points on the centerline, generating parameter functions over the centerline pixel index. This enables the production of multiple distance, time, and area values for each pair of points. In this work, two methods are compared for reducing uncertainty in the data obtained. One method fits each parameter model separately and derives flow from these models, while the other fit models multiple parameters together and calculates the flow afterwards. A comparison of these methods is made with simulation.

Centerline Shortening. This method involves adjusting the starting point of the centerline while keeping the stopping point fixed, which allows for calculation of the three parameters for each point pair. Consequently, the parameters can be expressed as a function of the adjusted starting point, also called centerline pixel index. We define the upper left pixel of the centerline as $i = 1$ and the lower right $i = n$, where n is the total number of pixels on the centerline. The parameters $\Delta s_{x,n}$, $\Delta t_{x,n}$ and $A_{x,n}$ of each calculation method are evaluated separately:

– $\Delta s_{x,n}$ equals the length of subcurve from $i = x$ to $i = n$,
– $A_{x,n} = \frac{\pi}{4} \cdot \sum_{i=x}^{n} d_i^2$, see Equation 2,
– $\Delta t_{x,n}$: two IDCs based on pixel $i = x$ and $i = n$ are calculated and thus, two transit times.

x stands for the index of the starting pixel. As the used stopping pixel is always $i = n$, we do not include it in the following notations. $A(x)$ is expected to remain constant, while $\Delta s(x)$

should decrease over pixel index or increase over normalized selected centerline length, since it represents the arc length of a curve. Similarly, $\Delta t(x)$ is expected to increase over normalized centerline length since velocity is assumed to be constant. **Uncertainty Reduction.** The flow can be derived from the parameter functions expressed as a function of the centerline length. Although only one flow is usually needed in practical applications, expressing it as a function over the centerline length enables better comparison. The flow calculation procedure is performed as follows. **Method 1 – Direct Line Fitting:** $A(x)$ is fitted as a constant line, while $\Delta s(x)$ and $\Delta t(x)$ are fitted as two lines separately. Flow signal is then calculated through values of the three fitted lines over the centerline index. **Method 2 – Bounded Line Fitting:** $A(x)$ is again fitted as a constant line. $\Delta s(x)$ and $\Delta t(x)$ are, however, fitted as two lines together. All variables with hat notation now represent the expected continuous model. According to Equation 3, the condition $\frac{k_1}{k_2} \stackrel{!}{=} \frac{b_1}{b_2}$ has to be fulfilled, so that the velocity is independent of x. Both slopes need to be nonzero, otherwise the data are physically, physiologically or mathematically wrong. Thus,

$$\hat{v}(x) = \frac{k_1 x + b_1}{k_2 x + b_2} = \frac{k_1}{k_2} + \frac{b_1 - \frac{k_1}{k_2} b_2}{k_2 x + b_2} \stackrel{!}{=} c,\ b_1 - \frac{k_1}{k_2} b_2 \stackrel{!}{=} 0. \quad (3)$$

The ideal time curve can be written as $\Delta\hat{t}(x) = k_2 x + b_2 = k_2(x + b_1/k_1)$. The next step is to fit $\Delta\hat{s}(x)$ to obtain k_1, b_1 and fit $\Delta\hat{t}(x)$ to derive k_2. The Mean Square Error (MSE) is used as the metric. The error function $\epsilon(k_2)$ is given in Equation 4. To minimize the error, the first derivative of the error function over k_2 is calculated and set to zero according to Equation 5. After the calculation of k_2, we can simplify $\hat{v}$ as described in Equation 6. Afterwards, $A(x)$ is fit to a constant. Finally, the flow reads $\dot{V} = \hat{v}\hat{A}$. To realize a comparison between results after line fitting and centerline shortening, the flow is again written as function of pixel index according to Equation 7, where $\bar{A}$ is the mean value of all $A(x)$. This approximation is generally valid based on our test results. The corresponding equations then read:

$$\epsilon(k_2) = \sum_{x=1}^{n} \left(t_x - \hat{t}(x)\right)^2 = \sum \left(k_2 \left(x + \frac{b_1}{k_1}\right) - t_x\right)^2, \quad (4)$$

$$\frac{d\epsilon}{dk_2} = \sum (x + \frac{b_1}{k_1}) \cdot 2(k_2(x + \frac{b_1}{k_1}) - t_x) \stackrel{!}{=} 0, \quad (5)$$

$$k_2 = \frac{\sum t_x \left(x + \frac{b_1}{k_1}\right)}{\sum \left(x + \frac{b_1}{k_1}\right)^2},\ \hat{v} = \frac{k_1}{k_2} = \frac{\sum \hat{s}(x)^2}{\sum t_x \hat{s}(x)}, \quad (6)$$

$$\dot{V}_x = \hat{A}_x \frac{\sum_{i=x_0}^{n} \hat{s}(i)^2}{\sum_{i=x_0}^{n} t_i \hat{s}(i)} \approx \bar{A} \frac{\sum_{i=x_0}^{n} \hat{s}(i)^2}{\sum_{i=x_0}^{n} t_i \hat{s}(i)}. \quad (7)$$

Normalized centerline length is introduced to substitute x for better visualization. The formel can be easily derived in mind and thus will not present in this work.

A comparison of these two methods is made via simulations. As $A(x)$ is generally constant, it is set to $1\,\mathrm{m}^2$ in simulation. Blood flow is assumed to be $8\,\mathrm{ml/min}$ which is confirmed according to our patient data. $\Delta s(x)$ is set as a vector from $0.1\,\mathrm{cm}$ to $1\,\mathrm{cm}$ with step size $0.005\,\mathrm{cm}$. Time is noised using additive white Gaussian noise (AWGN) but with signal to noise ratio (SNR) ranging from 1 dB to 40 dB. AWGN can approximate the noise in $\Delta t(x)$ according to [7]. Then, two methods will be applied and the mean value of flow will be calculated over SNR of time. 10000 tests are made to each SNR.

4 Results

Centerline Shortening. Figure 3 and 4 visualize the centerline shortening results of $A(x)$, $\Delta s(x)$ and $\Delta t(x)$ on a exemplary patient. Here we use the normalized centerline length as variable. These graphics are generally valid for all patient data.

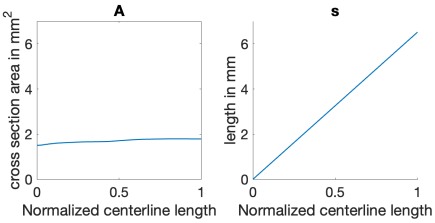

Fig. 3: Testing results of $A(x)$ and $\Delta s(x)$ using centerline shortening based on one exemplary patient in the same scalar.

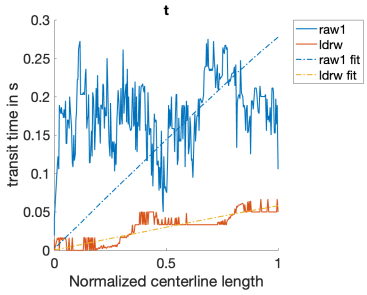

Fig. 4: Δt in origin and bounded fitting after centerline shortening in one exemplary patient.

Uncertainty Reduction. Figure 5 shows the comparison through simulation between direct and bounded line fitting. Figure 6 visualizes calculated flow signals of both methods using in vivo patient data.

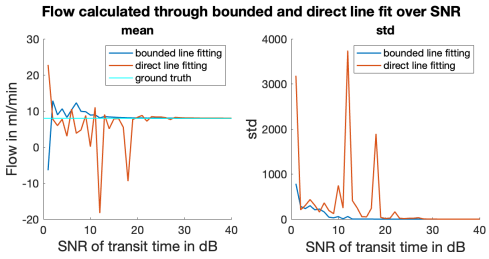

Fig. 5: Comparison of direct and bounded line fitting. Mean values (right) and standard deviation (left) of calculated velocity over SNR of Δt are visualized.

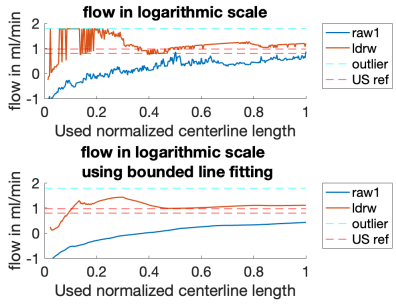

Fig. 6: Flow value without (top) or with (bottom) bounded line fitting after centerline shortening. The higher the used length, the more data are exploited in uncertainty reduction.

5 Discussion

Transit time is the most sensitive parameter and has a substantial impact on the calculated flow. Using centerline shortening, a large amount of data can be obtained. Note that centerline shortening must be combined with line fitting. Furthermore, not all data generated via centerline shortening should be used, as discretization errors may occur if at least one data value is too small. This is the case e.g., when Δs is smaller than three pixels, see Figure 3. Bounded line fitting is more suitable than separate line fitting both in terms of accuracy and deviation, according to Figure 5. High SNR difference between Δs and Δt is ideal, as it adds information to noisy signals. Besides, our approach needs only little time comparing to whole QFA execution duration. Thus it is suitable for intraoperative usage. Finally, our method is generally valid for all transit time calculation methods.

6 Conclusion and Outlook

Using centerline shortening and line fitting, uncertainty of flow measurement can be reduced even if its source and distribution is unclear. Bounded line fitting works generally better than direct line fitting based on simulation results. In our application, centerline shortening can be advanced to the two-dimensional case where signals depend on any pixel pair on the centerline instead of only the start pixel. In this case, accuracy should be even higher.

Author Statement

Research funding: The author state no funding involved. Conflict of interest: Authors state no conflict of interest. Informed consent: Informed consent has been obtained from all individuals included in this study. Ethical approval: The research related to human use complies with all the relevant national regulations, institutional policies and was performed in accordance with the tenets of the Helsinki Declaration, and has been approved by the authors' institutional review board or equivalent committee.

References

[1] Bullmore E, Sporns O. The economy of brain network organization. Nat Rev Neurosci 2012;13:336–349.

[2] Awano T, Sakatani K, Yokose N, Kondo Y, Igarashi T, Hoshino T et al. Intraoperative ec-ic bypass blood flow assessment with indocyanine green angiography in moyamoya and non-moyamoya ischemic stroke. World Neurosurgery 2010;73(6):668-674.

[3] Yamaguchi K, Kawamata T, Kawashima A, Hori T, and Okada Y. Incidence and predictive factors of cerebral hyperperfusion after extracranial-intracranial bypass for occlusive cerebrovascular diseases. Neurosurgery 2010;67(6):1548:1554.

[4] Amin-Hanjani S, Meglio G, Gatto R, Bauer A, Charbel F. T. The utility of intraoperative blood flow measurement during aneurysm surgery using an ultrasonic perivascular flow probe. Neurosurgery 2008;62(6):1346-1353.

[5] Nakamura A, Kawashima A, Nomura S, Kawamata T. Measurement of intraoperative graft flow predicts radiological hyperperfusion during bypass surgery in patients with moyamoya disease. Cerebrovasc Dis Extra 2020;10(2):66-75.

[6] Naber A. Intraoperative, Quantitative, and Non-Contact Blood Volume Flow Measurement via Indocyanine Green Fluorescence Angiography. PhD thesis, Karlsruher Institut für Technologie (KIT), 2021.

[7] Naber A, Reiß M, and Nahm W. Transit time measurement in indicator dilution curves: Overcoming the missing ground truth and quantifying the error. Frontiers in Physiology 2021;12.

[8] MATLAB. *version 9.10.0 (R2021a)*. The MathWorks Inc., Natick, Massachusetts, 2021.